

The hadronic contribution to the running of the electromagnetic coupling and the electroweak mixing angle

Teseo San José ^{c,d,e} ¹ Marco Cè ^a Antoine Gérardin ^b Georg von Hippel ^{d,e}
Harvey B. Meyer ^{c,d,e} Kohtaroh Miura ^{c,d,f} Konstantin Ottnad ^{d,e}
Andreas Risch ^g Jonas Wilhelm Hartmut Wittig ^{a,c,d,e}

^aCERN, Department of Theoretical Physics, Geneva, Switzerland

^bAix-Marseille-Universität, Université de Toulon, CNRS, CPT, Marseille, France

^cHelmholtz-Institut Mainz, Johannes Gutenberg-Universität Mainz, Germany

^dPRISMA⁺ Cluster of Excellence, Johannes Gutenberg-Universität Mainz, Germany

^eInstitut für Kernphysik, Johannes Gutenberg-Universität Mainz, Germany

^fKobayashi-Maskawa Institute for the Origin of Particles and the Universe, Nagoya University, Japan

^gDESY, John von Neumann Institute for Computing (NIC), Zeuthen, Germany

Lattice Conference, 27/07/2021

The QED running coupling $\alpha(q^2)$:

- $\alpha(M_Z^2)$ is an input quantity in electroweak global fits.
- Closely related to a_μ^{HLO} . Both can be obtained from the R-ratio data, $\sigma(e^+e^- \rightarrow \text{hadrons})/\sigma(e^+e^- \rightarrow \mu^+\mu^-)$ [Davier et al. 2020; Jegerlehner 2020; Keshavarzi, Nomura, and Teubner 2020], and the optical theorem.
- The future experiment MUonE (CERN) [Abbiendi et al. 2017] will compute a_μ^{HLO} from the running coupling via a dispersion integral.

The weak mixing angle $\sin^2 \theta_W$:

- It is a probe for BSM physics in many low energy $q^2 \ll M_Z^2$ experiments:
 - ▶ Neutrino cross-section scattering.
 - ▶ Parity-violating lepton scattering.
 - ▶ Parity-violating atomic experiments.
- Target of new experiments to improve precision at low energies, like P2 at MESA [Becker et al. 2018], and MOLLER and SoLID at JLab [Souder 2016; Benesch et al. 2014; Chen et al. 2014].
- To obtain it from experiment one needs to perform *flavour separation*, which is an extra systematic uncertainty.

The uncertainties of both are dominated by hadronic effects. In this work we use methods similar to those used to compute a_μ [Gérardin et al. 2019].

Main definitions

The hadronic contribution to $\alpha(Q^2)$ is defined with an effective coupling in the *on-shell* scheme,

$$\alpha(q^2) = \frac{\alpha}{1 - \Delta\alpha(q^2)},$$

with α the fine-structure constant. We study

$$(\Delta\alpha)_{\text{had}}(q^2) = 4\pi\alpha\hat{\Pi}^{\gamma\gamma}(q^2).$$

The hadronic contribution to $\sin^2\theta_W$ is, to leading order, [Burger et al. 2015; Jegerlehner 1986]

$$(\Delta\sin^2\theta_W)_{\text{had}}(q^2) = -\frac{4\pi\alpha}{\sin^2\theta_W}\hat{\Pi}^{Z\gamma}(q^2),$$

with $\sin^2\theta_W$ the equivalent of the fine-structure constant. The superscript γ refers to the electromagnetic current,

$$j_\mu^\gamma = \frac{2}{3}\bar{u}\gamma_\mu u - \frac{1}{3}\bar{d}\gamma_\mu d - \frac{1}{3}\bar{s}\gamma_\mu s + \frac{2}{3}\bar{c}\gamma_\mu c + \dots,$$

and Z to the vector part of the neutral weak current,

$$j_\mu^Z|_{\text{vector}} = j_\mu^{T_3}|_{\text{vector}} - \sin^2\theta_W j_\mu^\gamma,$$

with

$$j_\mu^{T_3}|_{\text{vector}} = \frac{1}{4}\bar{u}\gamma_\mu u - \frac{1}{4}\bar{d}\gamma_\mu d - \frac{1}{4}\bar{s}\gamma_\mu s + \frac{1}{4}\bar{c}\gamma_\mu c + \dots,$$

The main expression is

$$\hat{\Pi}(Q^2) = \int_0^\infty dt G(t) K(t, Q^2), \quad \text{with} \quad K(t, Q^2) = t^2 - \frac{4}{Q^2} \sin^2 \left(\frac{Qt}{2} \right).$$

Any Q^2 can be input to the kernel, but

- $Q^2 \sim (\pi/a)^2$ yield strong cut-off effects.
- $Q^2 \ll 1 \text{ GeV}^2$ weight more the data noise at long distances.

The correlators $G^{\gamma\gamma}(t)$ and $G^{Z\gamma}(t)$ are expressed in an isospin basis plus the charm-quark component,

$$G^{\gamma\gamma}(t) = G^{33}(t) + \frac{1}{3} G^{88}(t) + \frac{4}{9} G^{cc}(t),$$

$$G^{Z\gamma}(t) = \left(\frac{1}{2} - \sin^2 \theta_W \right) G^{\gamma\gamma}(t) - \frac{1}{6\sqrt{3}} G^{08}(t) - \frac{1}{18} G^{cc}(t).$$

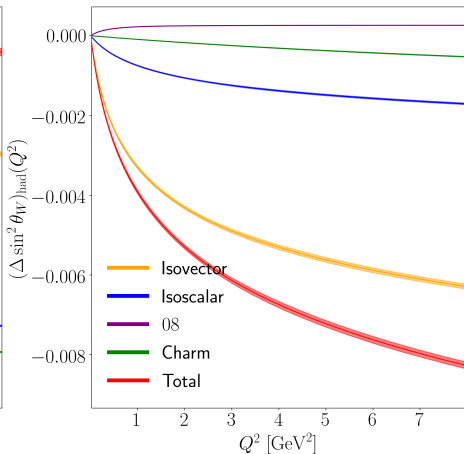
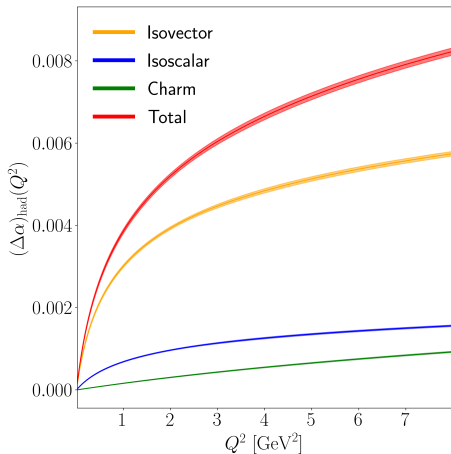
The isovector, isoscalar and 08 components have the flavour combinations

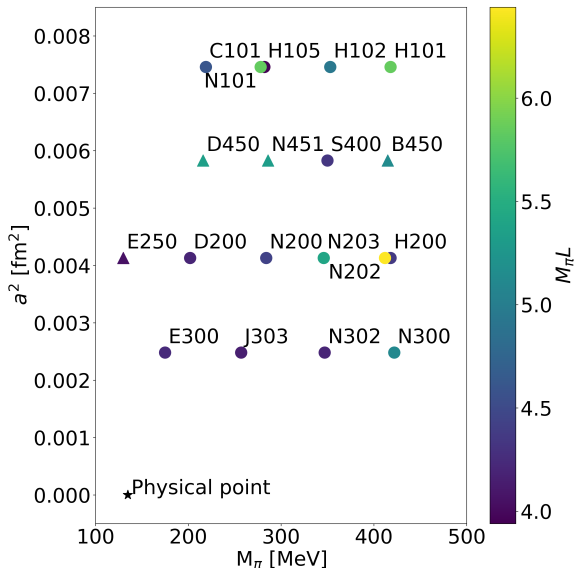
$$G^{33}(t) = \frac{1}{2} C^{\ell,\ell}(t),$$

$$G^{88}(t) = \frac{1}{6} \left(C^{\ell,\ell}(t) + 2C^{s,s}(t) + 2D^{\ell-s,\ell-s}(t) \right),$$

$$G^{08}(t) = \frac{1}{2\sqrt{3}} \left(C^{\ell,\ell}(t) - C^{s,s}(t) + D^{2\ell+s,\ell-s}(t) \right).$$

$\Delta\alpha$ and $\Delta\sin^2\theta_W$ vs energy





Signal-to-noise ratio

- ▶ We use the bounding method to improve the signal. [Gérardin et al. 2019; Borsanyi et al. 2018].

Finite-size effects

- ▶ We compare two methods: the MLL method [Harvey B. Meyer 2011; Lellouch and Luscher 2001; Luscher 1991] with GS $F_\pi(Q^2)$ parameterisation [Gounaris and Sakurai 1968], and the Hansen-Patella method [Hansen and Patella 2020, 2019].

Extrapolation to the physical point

- ▶ Similar approach to a_μ^{HLO} [Gérardin et al. 2019].
- ▶ Its uncertainty lies between 0.5% and 1%.

QED and strong isospin breaking corrections

- ▶ Some ensembles are already processed. Work in progress. [Risch and Wittig 2019, 2018a,b]
- ▶ The effect is $< 1\%$ for $\Delta\alpha$, and $\sim 0.1\%$ for $\Delta\sin^2\theta_W$. Less relevant at high energies.

Scale setting uncertainty

- ▶ We use the scale $\sqrt{8t_0^{\text{phy}}} = 0.415(4)(2)$ fm. [Bruno, Korzec, and Schaefer 2017]
- ▶ $\hat{\Pi}$ is dimensionless. The scale enters indirectly through the energy $8t_0^{\text{phy}} Q^2$, and the physical point $\phi_2^{\text{phy}} = 8t_0^{\text{phy}} (M_\pi^{\text{phy}})^2$, $\phi_4^{\text{phy}} = 8t_0^{\text{phy}} \left((M_\pi^{\text{phy}})^2/2 + (M_K^{\text{phy}})^2 \right)$.
- ▶ We estimate this error using bootstrap. Its size is $\sim 0.5\%$.

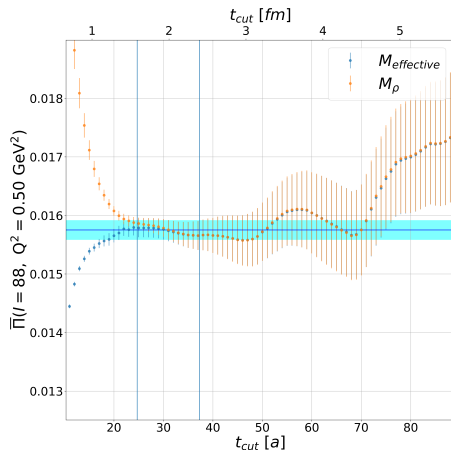
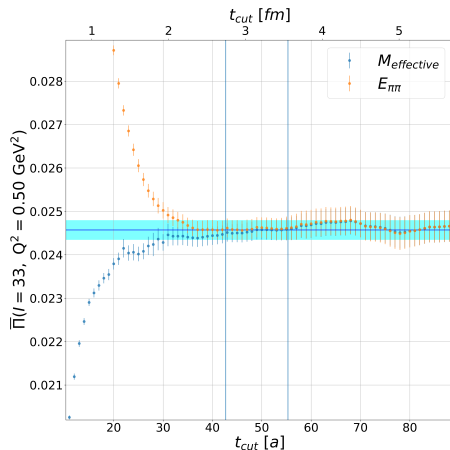
Rational approximation of the running [Aubin et al. 2012]

Signal-to-noise ratio problem

We can bound a correlator with positive spectral decomposition with the effective mass $M_{\text{eff}}(x_0) = \log [G(x_0)/G(x_0 + 1)]$, and the ground-state energy E_0 , [Borsanyi et al. 2018]

$$0 \leq G(x_0^{\text{cut}}) e^{-M_{\text{eff}}(x_0)(x_0 - x_0^{\text{cut}})} \leq G(x_0) \leq G(x_0^{\text{cut}}) e^{-E_0(x_0 - x_0^{\text{cut}})}, \quad x_0 \geq x_0^{\text{cut}}$$

Example at M_π^{phy} :



We use $t_i = \left(\frac{M_\pi L}{4}\right)^2 / M_\pi$ to estimate when a handful of states can describe the spectral representation of the correlator.

- At $t < t_i$, we employ the HP method [Hansen and Patella 2020, 2019], which computes the correction as an expansion in the squared momentum vector, $\vec{n}^2 = 1, 2, 3, 6, \dots$, with each term of order $\exp\{-|\vec{n}|M_\pi L\}$.
- At $t \geq t_i$, we employ the MLL method [Harvey B. Meyer 2011; Lellouch and Luscher 2001; Luscher 1991] with the GS parameterisation [Gounaris and Sakurai 1968]. The HP method gives compatible results with the MLL procedure at long distances, albeit the former is systematically smaller.

The method describes the finite-volume correlator as

$$G(t, L) = \sum_n |A_n|^2 e^{-\omega_n t},$$

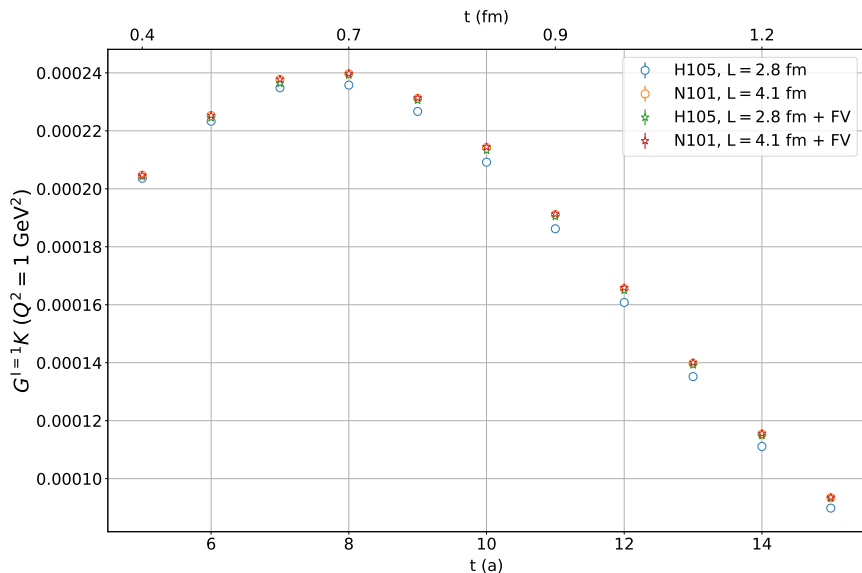
where $|A_n|^2$ is related to $F_\pi(Q^2)$ and the energy levels are related to the infinite-volume phase shifts.

The infinite-volume correlator is described via the continuous spectral representation

$$G(t) = \int_0^\infty d\omega \omega^2 \rho(\omega^2) e^{-\omega|t|}, \quad \rho(\omega^2) = \frac{1}{48\pi^2} \left(1 - \frac{4M_\pi^2}{\omega^2}\right)^{3/2} |F_\pi(\omega)|^2, \quad x_0 \neq 0.$$

We take $G(t) - G(t, L)$ to estimate the finite-size correction.

Finite-size correction. H105 vs N101



Finite-size corrections are $\sim 2\%$ in H105, but only 0.2% in N101.

Extrapolation to the physical point. Fit models

We perform a combined extrapolation to the physical point [Blum et al. 2021; Zyla et al. 2020]

$$a \rightarrow 0, \quad M_\pi^{\text{phy}} = 134.9768(5) \text{ MeV}, \quad M_K^{\text{phy}} = 495.011(15) \text{ MeV}.$$

We use the dimensionless variables [Bruno, Korzec, and Schaefer 2017]

$$a^2/8t_0^{\text{sym}}, \quad \phi_2 = 8t_0 M_\pi^2, \quad \phi_4 = 8t_0(M_\pi^2/2 + M_K^2).$$

The isovector and isoscalar components are extrapolated together. The model can be decomposed into $\hat{\Pi}_{33+88}(a, \phi_2, \phi_4) = \hat{\Pi}_{\text{continuum}}(a) + \hat{\Pi}_{\text{mass}}(\phi_2, \phi_4)$,

$$\hat{\Pi}_{\text{continuum}}(a) = \begin{cases} \hat{\Pi}^{\text{sym}} + \alpha_{2,d} (a^2/8t_0^{\text{sym}}) & \lesssim 2 \text{ GeV}^2, \\ \hat{\Pi}^{\text{sym}} + \alpha_{2,d} (a^2/8t_0^{\text{sym}}) + \alpha_{3,d} (a^2/8t_0^{\text{sym}})^{3/2} & \gtrsim 2 \text{ GeV}^2, \end{cases}$$

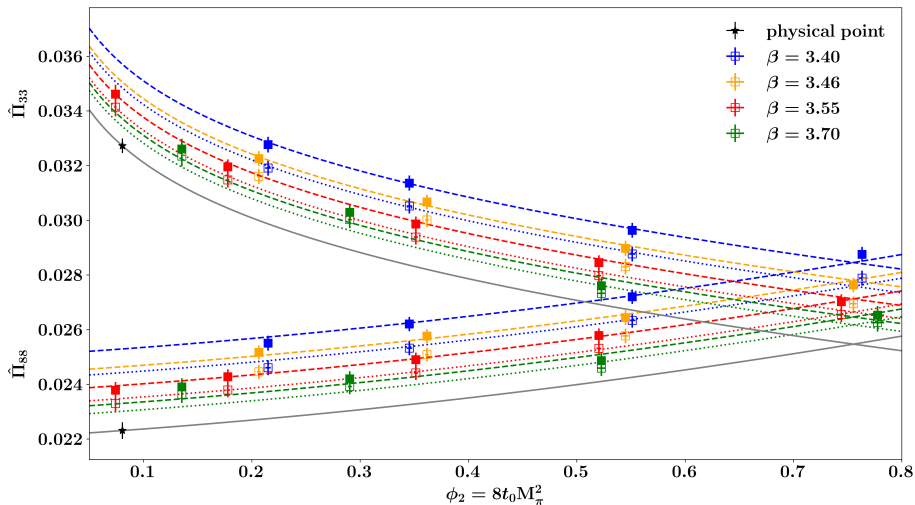
The mass dependency changes with isospin. For the isovector and isoscalar, we use

$$\hat{\Pi}_{\text{mass}}(\phi_2, \phi_4) = \beta_{1,i} (\phi_2 - \phi_2^{\text{sym}}) + \delta \left(\phi_4 - \frac{3}{2} \phi_2^{\text{sym}} \right) + \beta_{2,i} \begin{cases} \log(\phi_2/\phi_2^{\text{sym}}), \\ (\phi_2 - \phi_2^{\text{sym}})^2. \end{cases}$$

For the charm contribution, $\hat{\Pi}_{\text{charm}}(a, \phi_2) = \hat{\Pi} + \alpha_{2,d} (a^2/8t_0^{\text{sym}}) + \beta_{1,c} (\phi_2 - \phi_2^{\text{sym}})$.

For the 08 component, we use simply $\hat{\Pi}_{08}(M_\pi, M_K) = \hat{\Pi} 8t_0^{\text{sym}} (M_K^2 - M_\pi^2)$.

Isoscalar + isoscalar extrapolation at 1 GeV^2



- We compute the hadronic contributions to the running of $\alpha(Q^2)$, and $\sin^2 \theta_W(Q^2)$ in the interval $(0, 7] \text{ GeV}^2$.
- The total uncertainty varies between 2% at small energies, to 1% beyond $Q^2 \sim 1 \text{ GeV}^2$.
- Comparison with different phenomenological estimates is in progress. [Davier et al. 2020; Jegerlehner 2020; Keshavarzi, Nomura, and Teubner 2020]
- QED and strong isospin breaking effects are still under computation. [Risch and Wittig 2019, 2018a,b]
- Next, my colleague Kohtaroh Miura will explain how to use these results to compute $\Delta\alpha^{(5)}(M_Z^2)$.

Thank you for your attention!

	T/a	L/a	t_0^{sym}/a^2	a [fm]	L [fm]	M_π, M_K [MeV]	$M_\pi L$	# cnfg (con., dis., charm)		
H101	96	32	2.86	0.08636	2.8	418	5.9	2000	-	1000
H102	96	32			2.8	353 438	4.9	1900	1900	997
H105*	96	32			2.8	281 463	3.9	1000	1000	500
N101	128	48			4.1	279 461	5.9	1155	1155	350
C101	96	48			4.1	219 470	4.6	2000	2000	400
B450	64	32	3.659	0.07634	2.4	414	5.1	1600	-	800
S400	128	32			2.4	351 441	4.3	1720	1720	800
N451	128	48			3.7	286 460	5.3	1000	1000	200
D450	128	64			4.9	216 475	5.3	500	500	300
H200*	96	32	5.164	0.06426	2.1	418	4.4	1980	-	500
N202	128	48			3.1	411	6.4	875	-	450
N203	128	48			3.1	345 442	5.4	1500	1500	700
N200	128	48			3.1	283 462	4.4	1695	1695	400
D200	128	64			4.1	201 480	4.2	2000	2000	500
E250	192	96			6.2	129 489	4.1	485	485	65
N300	128	48	8.595	0.04981	2.4	422	5.1	1680	-	500
N302	128	48			2.4	346 451	4.2	2190	2190	500
J303	192	64			3.2	257 474	4.2	1040	1040	100
E300	192	96			4.8	175 491	4.2	600	600	100

* only used in the estimation of finite-size effects.

	aM_π	aM_ρ ^[2]	$aE_{\pi\pi}$	$aE_{\pi\pi\pi}$ ^[3]
H101	0.1830 (5)	0.3749 (15)	0.5427 (6)	0.8695 (9)
H102	0.1546 (5)	0.3683 (19)	0.5076 (6)	0.8177 (9)
H105	0.1234 (13)	0.3373 (94)	0.4799 (52)	0.7677 (19)
N101	0.1222 (5)	0.3339 (38)	0.3713 (20)	0.5799 (10)
C101	0.0960 (6)	0.3260 (35)	0.3090 (16)	0.5332 (10)
B450	0.1605 (4)	0.3360 (15)	0.5135 (5)	0.8280 (7)
S400	0.1358 (4)	0.3235 (25)	0.4863 (6)	0.7866 (7)
N451	0.1108 (3)	0.3011 (27)	0.3517 (4)	0.5588 (5)
D450	0.0836 (4)	0.2962 (19)	0.2536 (5)	0.4199 (7)
H200	0.1363 (5)	0.2933 (27)	0.4909 (18)	0.7874 (7)
N202	0.1342 (3)	0.2830 (14)	0.3785 (4)	0.6035 (6)
N203	0.1124 (2)	0.2678 (30)	0.3506 (3)	0.5617 (4)
N200	0.0922 (3)	0.2521 (34)	0.3280 (3)	0.5271 (4)
D200	0.0655 (3)	0.2516 (20)	0.2277 (8)	0.3896 (4)
E250	0.0422 (2)	0.2515 (40)	0.1546 (3)	0.2575 (4)
N300	0.1067 (3)	0.2238 (20)	0.3420 (5)	0.5513 (6)
N302	0.0875 (3)	0.2150 (29)	0.3207 (4)	0.5197 (5)
J303	0.0649 (2)	0.2005 (43)	0.2423 (10)	0.3886 (3)
E300	0.0442 (1)	0.1971 (24)	0.1555 (5)	0.2606 (2)

²Andersen et al. 2019.

³Hansen, Romero-López, and Sharpe 2020.